Characterization of optical fibers using multiscale X-ray Computed Tomography

Journal of Physics: Conference Series **3294** (2026) 012007 doi:10.1088/1742-6596/3294/1/012007

Characterization of optical fibers using multiscale X-ray Computed Tomography

M.C. Crocco[1,2] F. Cognigni[3,4], A. Sanna[3], R. Filosa[1], S. Siprova[2], R.C. Barberi[1,2], R.G. Agostino[1,2], J.J. Beltrano[1], S. Wabnitz[5], A. D'Alessandro[5], C. Santini[5], S. Lebrun[6], M. Rossi[3], V. Formoso[1,2], R. Termine[2], A. Bravin[1,2,7,8] and M. Ferraro[1,2]

[1]Department of Physics and STAR Research Infrastructure, University of Calabria, Rende (CS), Italy
[2]CNR-NANOTEC (SS di Rende), Rende (CS), Italy
[3]Department of Basic and Applied Sciences for Engineering (SBAI), University of Rome La Sapienza, Rome, Italy
[4]Carl Zeiss S.p.A, Research Microscopy Solutions, Milan, Italy
[5]Department of Information Engineering, Electronics, and Telecommunications, Sapienza University of Rome, Rome, Italy
[6]Institut d'Optique Graduate School, CNRS, Laboratoire Charles Fabry, Université Paris-Saclay, Palaiseau, France
[7]Department of Physics, "G. Occhialini", University Milano Bicocca, Milan, Italy
[8]European Synchrotron Radiation Facility, Grenoble, France

E-mail: mariacaterina.crocco@unical.it

Abstract. X-ray computed tomography (XCT) has emerged in recent years as a non-destructive technique for the 3D characterization of optical fibers, enabling the spatial mapping of refractive index variations and the evaluation of geometric parameters. This paper presents a multiscale characterization of standard optical fibers based on three XCT approaches with different resolutions. In particular, our results show the presence of a previously unreported parabolic profile in a single-mode optical fiber sample and demonstrate how the core/cladding ratio in a fiber taper is nearly constant along the fiber axis. Generally speaking, our results show how the various techniques are suitable for studying different optical fibers and identify the most appropriate technique for different applications, such as laboratory and industrial.

1 Introduction

Optical fibers are a key enabling technology for modern photonics, with applications spanning telecommunications, medical diagnostics, sensing, and nonlinear optics. Their operation relies on precise control of the refractive index contrast between the core and the cladding, typically achieved by selective doping of silica-based material. As fiber designs become increasingly complex, including specialty fibers, tapers, and nanofibers, accurate and spatially resolved characterization of their internal structure and refractive index distribution becomes essential.

Despite significant advances in fiber fabrication, comprehensive characterization remains a challenge [1]. Most conventional techniques probe only the fiber end-face, providing limited information on possible longitudinal variations of the refractive index profile induced during the drawing process [2, 3, 4, 5, 6]. In contrast, transverse methods allow access to axial inhomogeneities, which are crucial for quality control and process optimization [7, 8, 9, 10, 11, 12].

Among transverse approaches, X-ray-based techniques have emerged as powerful non destructive tools. Small-angle X-ray scattering enables the investigation of structural features [13, 14, 15, 16], while X-ray computed tomography (XCT) provides three-dimensional imaging of fiber geometry and internal composition [17, 18, 19, 20]. Under conditions of contrast-absorption, the intensity of XCT can be correlated with the density of the material and the concentration of the dopant, allowing for indirect reconstruction of refractive index profiles [20, 21, 22, 23, 24]. This capability makes XCT particularly attractive for quantitative fiber characterization, even in the presence of coatings, bending, or multimaterial architectures.

However, a single XCT modality cannot simultaneously provide high spatial resolution, a large field of view, and rapid acquisition. Computed microtomography (μCT) offers wide imaging volumes but limited resolution, computed nanotomography (nCT) achieves nanometric detail over very small regions, and X-ray microscopy (XRM) represents an intermediate regime [24].

Here, we present a systematic multiscale investigation of standard optical fibers using three XCT techniques: μCT, XRM and nCT. By benchmarking their performance in terms of spatial resolution, field of view, acquisition efficiency, and segmentation robustness, we establish practical guidelines for selecting the optimal approach depending on fiber size and application requirements. Each XCT technique has specific advantages: μCT for analyzing long optical fibers, nCT for nanoscale structures, and XRM for optical fibers with small cores. Using XCT analysis, we found that the SMF optical fiber samples have a gradual distribution of the absorption profile, thus reflecting into a parabolic-like refractive index. This characteristic is clearly resolved thanks to the high spatial resolution of the XRM and nCT techniques. Furthermore, the study of the SMF fiber taper showed that the tapering process preserves the proportionality between the core and the cladding size along the fiber axis, at least within the nCT field of view (FOV). This result, which provides direct experimental confirmation of the high degree of geometric control that is achievable in fiber manufacturing processes, is pivotal for the design of optical nanofibers as well as for numerical simulations of nonlinear beam dynamics [25, 26].

2 Materials and Methods

The experimental study was conducted on widely used commercial optical fibers: a single-mode fiber (SMF) and two multimode fibers, one with a step-index (STEP) and the other with a graded-index (GRIN) profile respectively. These samples are representative of different refractive index architectures and doping configurations (Germanium and Fluorine), which influence X-ray absorption contrast. In addition, an SMF fiber taper, made by controlled thinning, was analyzed.

XCT acquisitions were performed using three different experimental configurations:

- μCT, characterized by a large field of view (FOV) and micrometric resolution [27];
- XRM, which allows sub-micrometric resolutions on volumes of the order of millimeters [28];
- nCT, capable of achieving resolutions on the order of 50 nm, but with a very limited field of view

For acquisition parameters and further details on the fibers analyzed and different XCT devices, see [24].

The images were reconstructed using Feldkamp-Davis-Kress algorithms [29] and then analyzed with dedicated software for tomographic image processing (Fiji ImageJ, Dragonfly 3D World 2024.1) [30]. Once the relevant information had been extracted, the obtained data was plotted using IgorPro 9.

3 Results

First step in XCT analysis is the 3D visualization of the various optical fibers (Fig. 1). By analyzing the 3D rendering and their relative 3D intensity profiles, we can easily see that the optical fibers have different characteristics.

In particular, the STEP fiber (Fig. 1a,b) has a significantly uniform XCT intensity profile in the core, consistent with a step refractive index. The GRIN fiber (Fig. 1c,d), on the other hand, shows a gradual variation in intensity from the center to the cladding, indicative of a parabolic index profile. The SMF fiber (Fig. 1e,f) shows a gradual core profile that is not explicitly reported in the manufacturer's specifications. In both STEP and SMF fibers, the presence of an intermediate layer (trench) was also identified between the core and the cladding.

Furthermore, nCT measurements on the SMF taper (Fig. 2) allowed us to observe a parabolic core profile in great detail and confirm the presence of the trench.

Once we observed the absorption differences between the various optical fibers, we compared techniques with different resolutions.

Figure 3a-c shows a comparison between the μCT (in green) and XRM (in violet) absorption profiles of different optical fibers. Focusing on the core, which is the region of greatest interest for studying the refractive index profile, we can see that the absorption profiles of STEP and GRIN fibers (Fig. 3a,b) are comparable. This result confirms the possibility of adequately profiling optical fibers even with micrometric resolution equipment. The result is different for SMF fiber (Fig. 3c), where, due to the small core (approximately 10 µm), micrometric techniques do not allow the absorption profile to be adequately resolved, while XRM does.

Figure 3d shows the absorption profile of the SMF taper acquired with nCT. Again, we can clearly see that the SMF fiber has a parabolic core profile, and we can also observe the presence of the trench more accurately.

At this point, the diameters of the core and the cladding were estimated. The values obtained with μCT and XRM (Table 1) are in very good agreement with those given by the manufacturers, with relative uncertainties typically less than 2%. In particular, we can observe that the cladding values for all fibers are around 125 μm, while the core diameters of STEP and GRIN fibers are approximately 50 μm, in accordance with the manufacture specs.

As for the SMF fiber, we were unable to determine the core diameter with the μCT, as our resolution is not sufficient. However, we were able to obtain a value very close to the manufacturer's value by analyzing the XRM data.

In the case of the SMF taper, the diameters were determined along the z-axis of the optical fiber, and the proportionality between the core and the cladding was experimentally verified

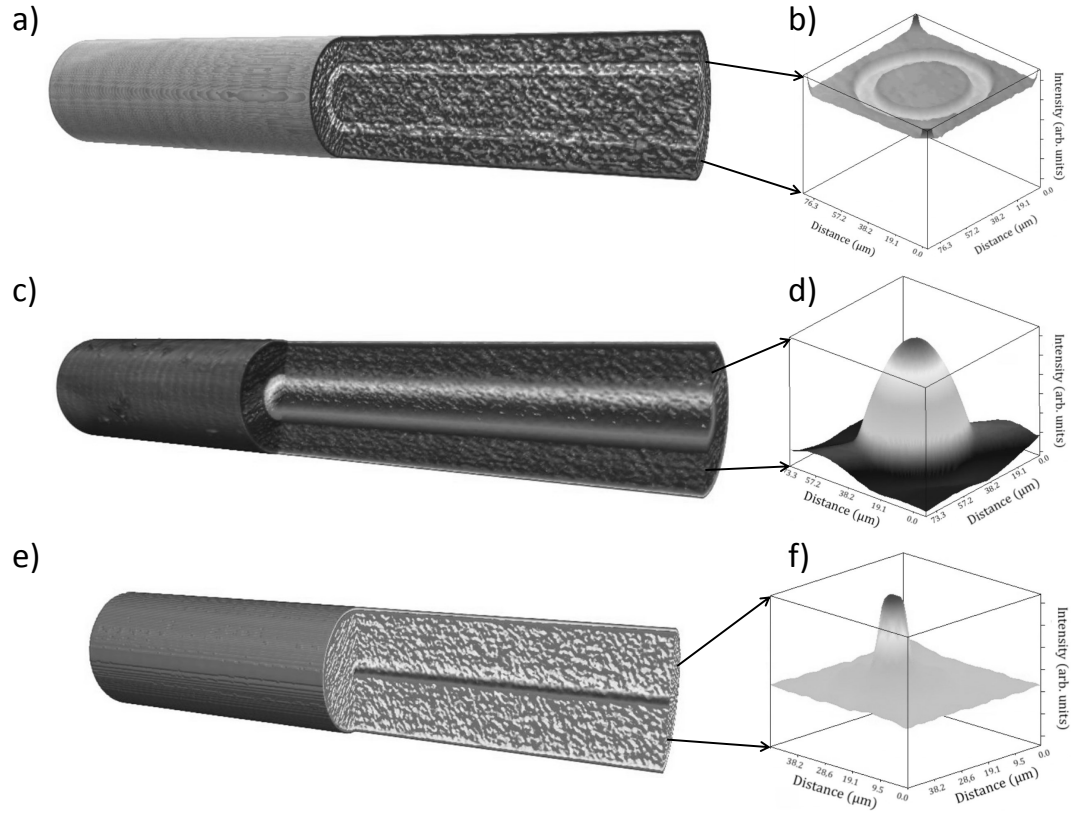

Figure 1: XRM results: 3D rendering of STEP (a), GRIN (c), and SMF (e) optical fibers. (b,d,f) 3D surface plot.

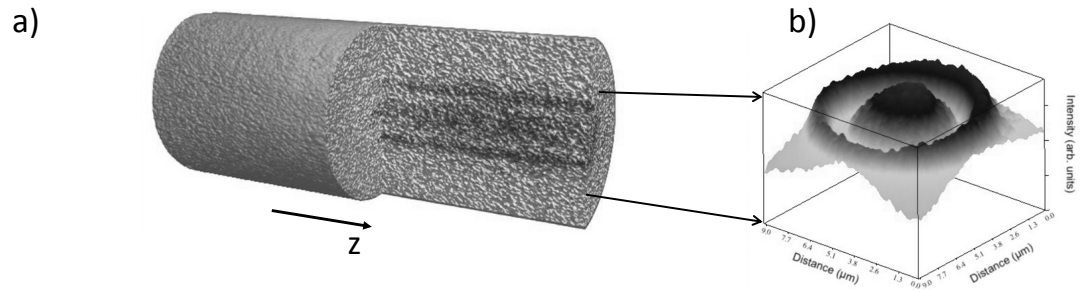

Figure 2: nCT results: (a) 3D rendering of taper, and (b) 3D surface plot.

(Table 2). For ease of reading, in Table 2, we report the diameter values at approximately 3 μm intervals. We can observe that, moving from the point at 0.00 μm to 23.04 μm, the diameters of the cladding and core are reduced from 22.46 μm to 22.27 μm and from 6.42 μm to 6.22 μm for the cladding and core, respectively.

However, this variation in diameter does not alter the proportional relationship between the cladding and the core. In fact, by determining the ratio between the two diameters (D_{clad}/D_{core}), we can easily see how this remains constant along the z-axis of the taper being analyzed (ap-

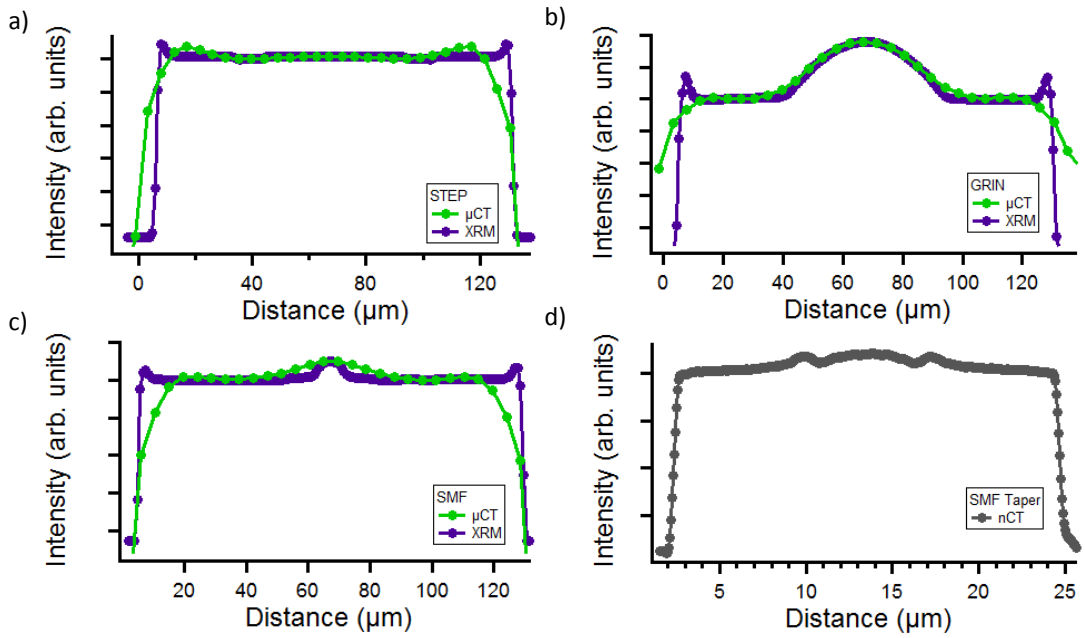

Figure 3: Comparison of intensity profiles for the STEP (a), the GRIN (b), and the SMF (c) optical fibers, respectively acquired whit μCT and XRM. (d) intensity profiles for the SMF taper acquired whit nCT.

	GRIN		STEP		SMF	
	D_{clad} (μm)	D_{core} (μm)	D_{clad} (μm)	D_{core} (μm)	D_{clad} (μm)	D_{core} (μm)
nominal	125.00	50.00	125.00	50.00	125.00	//
μCT	125.41	49.02	125.75	51.83	122.54	//
XRM	124.70	49.84	123.81	49.87	124.21	8.44

Table 1: Cladding and core diameters determined by XCT measurements, and comparison with the nominal value.

proximately 0.3).

z (μm)	D_{clad} (μm)	D_{core} (μm)	D_{clad}/D_{core}
0.00	22.46	6.42	0.29
3.20	22.44	6.43	0.29
7.04	22.40	6.36	0.28
10.24	22.37	6.31	0.28
13.44	22.35	6.26	0.28
16.64	22.32	6.26	0.28
19.84	22.29	6.28	0.28
23.04	22.27	6.22	0.28

Table 2: SMF taper diameters along z axes of the optical fiber determined by nCT measurements, and the proportionality value between the diameter of the cladding and that of the core.

Based on our results, we can claim that all XCT techniques used for this work are excellent

for analyzing both the absorption profile of different optical fibers and for obtaining geometric information. In particular, we can say that μCT is a useful technique for analyzing optical fibers with a large core, but also, due to its large field of view, fairly long optical fibers. On the other hand, XRM is a useful technique for studying optical fibers with a small core but small in length (a few millimeters). In perspective, the use of this technique can be extended to microstructured optical fibers. Finally, although the field of view and beam energy are very small (FOV about 64 μm and X-ray energy 5.4 keV), nCT is a technique that allows to investigate nano-optical fibers, permitting visualization and analysis of small structures (100-200 nm).

These different characteristics make the techniques suitable for characterizing optical fibers in various applications, whether in laboratories, manufacturing, or industry.

All of this can be made more accessible and easier by integrating XCT techniques with artificial intelligence (AI) applications, allowing real-time analysis during the production process by reducing acquisition, processing, and analysis times, as demonstrated in [24].

4 Conclusions

In conclusion, our results show the structural differences between various types of optical fibers. We were able to provide information on the absorption index profile and derive some geometric parameters such as the core and the cladding size. Our results show the presence of previously unnoticed features: a bell-shaped absorption profile in the core of a SMF optical fiber and the presence of a trench layer in both single- and multi-mode fibers. These observations were enabled by the high spatial resolution of the XCT techniques used. Furthermore, the study of the SMF fiber taper demonstrated that the tapered process preserves the geometric proportionality between the core and the cladding along the fiber axis. In the future, the combined XCT–AI approach paves the way for real-time quality monitoring systems and more robust and optimized production strategies for next-generation optical fibers.

Funding and acknowledgements

We acknowledge the support of the Italian Ministry of University and Research grant Progetto STAR 2, PIR01-00008 and the "Advanced Tomography and Microscopies" (ATOM) Project, granted by Lazio Region (Prot. #173-2017-17395 L.R. 13/2008), Regional call "Open Infrastructures for Research", the Piano Nazionale di Ripresa e Resilienza. (PNRR)—Research Infrastructure Project iENTRANCEENL (www.ientrance.eu) "Infrastructure for Energy Transition and Circular Economy EuroNanoLab" granted by Italian Ministry of University and Research (MUR), (Prot #IR0000027, call 3264, Dec. 28 2021), and the European Union – Next Generation EU in the framework of the National Recovery and Resilience Plan through the research project I-PHOQS - Integrated Infrastructure Initiative in Photonic and Quantum Sciences (B53C22001750006).

References

[1] Stewart W 2003 *IEEE Transactions on Microwave Theory and Techniques* **30** 1439–1454

[2] Ikeda M, Tateda M and Yoshikiyo H 1975 *Applied Optics* **14** 814–815

[3] Presby H, Mammel W and Derosier R 1976 *Review of Scientific Instruments* **47** 348–352

[4] Weng C J, Hsu K Y and Chen Y F 2015 *Optics Express* **23** 11755–11762

[5] Young M 1981 *Applied optics* **20** 3415–3422

[6] Zhong Q and Inniss D 1994 *Journal of lightwave technology* **12** 1517–1523

[7] Sochacka M 1994 *Journal of lightwave technology* **12** 19–23

[8] Barty A, Nugent K, Paganin D and Roberts A 1998 *Optics Letters* **23** 817–819

[9] Yablon A D 2009 *Journal of Lightwave Technology* **28** 360–364

[10] Bachim B L and Gaylord T K 2005 *Applied optics* **44** 316–327

[11] Gorski W and Osten W 2007 *Optics letters* **32** 1977–1979

[12] Fan S, Smith-Dryden S, Li G and Saleh B 2020 *Optics Express* **28** 6846–6858

[13] Beckers M, Vad T, Mohr B, Weise B, Steinmann W, Gries T, Seide G, Kentzinger E and Bunge C A 2017 *Polymers* **9** 60

[14] Lee S I, Seo M G, Huh J and Paik H j 2022 *Polymers* **14** 5567

[15] Perret E, Jakubowski K, Heuberger M and Hufenus R 2022 *Polymers* **14** 3262

[16] Ferraro M, Filosa R, Alamu Q, Kiedrowski K, Jupé M, Leonetti M, Wabnitz S, Marmiroli B, Barberi R, Formoso V *et al.* 2025 *Optical Materials* **162** 116856

[17] Sandoghchi S, Jasion G, Wheeler N, Jain S, Lian Z, Wooler J, Boardman R, Baddela N, Chen Y, Hayes J *et al.* 2014 *Optics Express* **22** 26181–26192

[18] Levine Z H, Peskin A P, Garboczi E J and Holmgren A D 2019 *Microscopy and Microanalysis* **25** 70–76

[19] Levine Z H, Garboczi E J, Peskin A P, Ekman A A, Mansfield E and Holm J D 2021 *Optics Express* **29** 1788–1804

[20] Ferraro M, Crocco M C, Mangini F, Jonard M, Sangiovanni F, Zitelli M, Filosa R, Beltrano J J, De Luca A, Barberi R C *et al.* 2022 *Optical Materials Express* **12** 4210–4222

[21] Crocco M C, Mangini F, Filosa R, Solano A, Agostino R G, Barberi R C, Couderc V, Klimczak M, Filipkowski A, Buczynski R *et al.* 2023 *Optical Materials Express* **14** 70–81

[22] Birks T A and Li Y W 2002 *Journal of lightwave technology* **10** 432–438

[23] Baker C and Rochette M 2011 *Optical Materials Express* **1** 1065–1076

[24] Crocco M C, Cognigni F, Sanna A, Filosa R, Siprova S, Barberi R C, Agostino R G, Wabnitz S, D'Alessandro A, Lebrun S *et al.* 2025 *Tomography of Materials and Structures* 100078

[25] Shan L, Pauliat G, Vienne G, Tong L and Lebrun S 2013 *Journal of the European Optical Society-Rapid publications* **8** 13030

[26] Zerbib M, Deroh M, Sylvestre T, Huy K P and Beugnot J C 2024 *APL Photonics* **9**

[27] `https://star.unical.it/star-lab/utomo/`

[28] `https://research.uniroma1.it/3d-x-ray-microscopy-xrm-zeiss-xradia-versa-610`

[29] Feldkamp L 1997 *J. Microsc.* **185** 67–75

[30] Schindelin J, Arganda-Carreras I, Frise E, Kaynig V, Longair M, Pietzsch T, Preibisch S, Rueden C, Saalfeld S, Schmid B *et al.* 2012 *Nature methods* **9** 676–682